ていたものの炎症細胞浸潤は認めなかった．OVA $_{323-339}$ ペプチドに対する T 細胞増殖反応と IFN-γ産生は高脂肪食摂取により減弱していたが，CD1d$^{-/-}$マウスでは明確な変化は見られなかった．高脂肪食摂取は EAU の臨床経過には影響を与えなかった．

【まとめ】高脂肪食摂取により NKT 細胞からの IFN-γ産生の減弱が見られ，OVA $_{323-339}$ ペプチドに対する T 細胞増殖反応の減弱が見られた．高脂肪食は NKT 細胞を介して獲得免疫系に影響をおよぼしうることが判明したが，その影響は実験モデルにより異なると考えられた．

インターフェロン・ベータ 1b 療法中止後の多発性硬化症治療について

分担研究者　小川　雅文　（国立精神・神経センター武蔵病院　神経内科）
研究協力者　山村　隆　（国立精神・神経センター神経研究所疾病研究第六部）

「はじめに」 多発性硬化症（MS）へのインターフェロン・ベータ 1b（IFN - β1b）療法をなんらかの理由で中止した例に、その後どのような治療がおこなわれているか検討した。

「患者と方法」 当院受診中の MS 患者 120 例から IFN - β1b 療法を導入された後に中止された例を抽出し後向き調査をおこなった。

「結果」 72 例中 15 例がなんらかの副作用のため IFN - β1b 療法を中止されていた。内訳は、導入後の再発部位の変化 2 例、導入直後の比較的重度の再発あるいは再発回数の増加 4 例、痙性の増悪 1 例、網膜静脈閉塞症 1 例、肝機能障害 1 例。皮膚症状 2 例、全身の倦怠感 1 例、精神症状 2 例、無効と主治医が判断して中止 1 例。さらに副作用はなかったが、挙児希望で 2 例が中止していた。全例で、IFN - β1b は漸減・中止されていた。

再発部位の変化や重度の再発あるいは再発回数の増加をみた例では、IFN - β1b 療法中止により症状は改善あるいはもとの病型に戻っていた。精神症状悪化例では中止により精神症状の改善をみていた。

IFN - β1b 療法中止後、再発をみた例はあったがあきらかに中止前より再発回数が増えた例はなかった。ただし今回の中止例以外に 1 例、自己判断で IFN - β1b 療法を一時的に中止した後 2 週目に右上肢麻痺を来たした例がありこの例については中止と再発の因果関係を否定できない。

IFN - β1b 療法中止後、5 例は再発時のステロイドパルス療法のみで新たな治療は追加されていなかった。他の例では重複を含み、免疫抑制剤 6 例、血漿吸着・交換 3 例、ステロイド少量経口投与 4 例、定期的なステロイドパルス療法 1 例、IVIG2 例を追加されていた。このなかで再発に関して、ステロイド少量経口投与が著効を示したと思われる例が 2 例あった。血漿吸着・交換は一定の症状の改善効果を示したが再発予防に有効であったかは判断が困難であった。なお IFN - β1b 療法による難治性の皮膚潰瘍には血漿吸着・交換が著効を示した。

「考察」 今回の検討では中止により再発回数の著増や、重症化した症例は認めなかった。（自己判断による中止例 1 例は除く） IFN - β1b 療法が使用できない例ではその後、様々な治療が選択されていたが現時点では特に優れているというものはなくカットアンドトライによる選択しかないと思われた。

「結論」 IFN - β1b が使用できない例について、どのような治療を選択すべきかなんらかの指標を立てる必要があると思われる。

日本における運動障害(movement disorder)を呈する多発性硬化症の特徴及びインターフェロンの効果に関する研究

分担研究者　○横山　和正
順天堂大学医学部脳神経内科

目的

多発性硬化症（MS）において movement disorder として不随意運動とパーキンソニズムが報告されている。不随意運動の多くは急性期の障害である action tremor, paroxysmal dystonia (tonic spasm)であり神経変性疾患などで多く認められる chorea, ballism, myoclonus, athetosis, sustained dystonia はまれである。またパーキンソニズムは lower body Parkinsonism であることが多いが、近年多発性硬化症において髄鞘のみならず神経細胞の障害も引き起きることが報告されることもあり炎症だけではなく神経変性の立場からの研究も進められている。インターフェロンの movement disorder を呈した MS に対する効果に関しては検討された報告はない。今回の我々の研究では当院に受診している MS 患者の神経障害部位、Parkinsonism, 不随意運動のパターンとその出現期間、治療に対する反応性について検討し少数ながらインターフェロン使用経験を報告する。

方法

高齢発症を 50 歳以上と定義した。多発性硬化症の診断は Poser's の診断基準を利用した。1986 年から 2006 年の間に、総計 203 名の患者の中から 13 例について検討した。既往歴、性別及び初発症状、病変の広がり、進行度、MRI、血液、髄液検査、治療に対する反応性について解析した。

結果

平均 EDSS は不随意運動を呈したグループで高値であった。

初発症状として不随意運動を呈したケースは認めなかった。

振戦の病巣との対応を MRI 上決定することはできなかった。振戦は持続することが多く ADL の障害となることが多かった。パーキンソン病の振戦と異なり下肢に認めることはまれであった。企図振戦は小脳症状も日本人には少ないためか認めなかった。Long cord lesion をもった多発性硬化症患者にはほぼ半数が不随意運動の出現を認めた。インターフェロンーβ療法はパーキンソニズムを呈した一症例に対して効果的であった。

結論

不随意運動に対する直接のインターフェロン効果は期待できないがパーキンソニズムの進展に関しては間接的に進行予防可能と考えた。

今後不随意運動陽性症例に対するインターフェロン使用例を蓄積し検討し神経変性の観点から研究を進める必要がある。

厚労省難治性疾患克服研究事業
「難治性疾患の画期的診断・治療法等に関する研究」班　分担研究

外傷をきっかけにした白質病変

分担研究者：太田　宏平[1)]
研究協力者：○ 大橋　高志[2)]、丸山　恵子[2)]、清水　優子[2)]、大原　久仁子[2)]、岩田　誠[2)]
1) 東京理科大学　理学部
2) 東京女子医科大学　神経内科

【目的】外傷を契機に多発性硬化症 (MS) が発症することが知られているが、外傷と MS の発症の関連についてはまだ十分な結論が出ていない。我々は頭部外傷後に大脳白質に脱髄と考えられる巨大病変が出現した症例を経験した。病変の形成には抗体や補体が強く関与している可能性があり、多発性硬化症の発症機序を考える上でたいへん興味深い。

【症例】患者は 59 歳の男性。大酒家でほぼ毎日泥酔するまで飲酒して帰宅していた。2005 年４月、飲酒後に酩酊状態で自転車に乗り転倒、右顔面を強打した。明らかな意識障害はなかった。第 37 病日から右下肢の感覚障害、第 47 病日からは右下肢の脱力が出現した。第 51 病日の頭部 CT で右慢性硬膜下血腫と左頭頂葉の巨大病変を認めたため、同日入院したが、入院後に右片麻痺が急速に増強した。頭部 MRI では、左頭頂葉の病変はリング状の enhancement を示した。ステロイドパルス療法を５クール施行したが、症状に明らかな改善はなかった。さらに、95 病日頃から急速に失語が進行病巣も拡大した。その後は、少しずつではあるが、症状は改善傾向になり、頭部 MRI では病巣は縮小傾向となった。

【考察】外傷を契機に MS が発症することは Charcot の時代から知られている。1901 年に Klausner は MS 症例 126 例のうち、24 例に外傷歴があることを報告している。その後、MS の発症の直前～１年以内に外傷歴がある患者が 10%前後いることが報告されている。1952 年に McAlpin は、外傷と MS に関して初めての case-controlled study を行い、MS 患者と正常者、各々250 名を調査したところ、MS 患者は対象に比べて発症３ヵ月前までの外傷の頻度が優位に多かったと報告している。その後の報告では相関がなかったとする報告がほとんどである。Retrospective study では recall bias がかかることや、統計学的な手法の問題点の指摘されており、外傷と MS の発症の関連についてはまだ十分な結論が出ていない。Lucchinetti らは、MS が病理学的に４型に分類できることを示し、そのうち第２型では脱髄巣における抗体、補体の沈着が特徴的であることを示した。このタイプでは特に病巣の辺縁にマクロファージの集積があり、MRI ではリング状に enhance されることも示されている。従って、本症例のようにリング状の enhancement を示す tumefactive region の形成には抗体や補体が強く関与している可能性があり、外傷後の脱髄病巣の形成機序を考える上で興味深いと考える。本症例は発症後、１年以上経過するが、その間には臨床的な再発や、MRI 上の新たな病巣の出現はなく、MS の診断には至っていない。今後、引き続き、経過を観察していく必要がある。

【結語】頭部外傷後に大脳白質に脱髄と考えられる巨大病変が出現した 59 歳男性例を経験した。症状は外傷後１ヶ月以上経過してから出現、病巣は３ヶ月以上かけて拡大・進展し、ステロイドパルス療法に抵抗性であった。脱髄巣の形成には抗体や補体が強く関与している可能性があり、多発性硬化症の発症機序を考える上で興味深いと考えた。

Arundic acid による再発性 EAE の抑制
-臨床経過および病理組織学的検討-

○富岳　亮、滝澤功一、井口貴子*、大貫　学*、高　昌星**、野村恭一*

埼玉医科大学 神経内科
埼玉医科大学総合医療センター　神経内科*
信州大学医学部保健学科生体情報検査学**

目的

Arundic acid（ONO-2506）は astrocyte の機能改善薬として近年開発され、現在、急性期脳血管障害の治療薬として注目されている。今回我々は、この ONO-2506 が多発性硬化症の治療薬としての可能性について検討するため、慢性進行型 EAE および再発寛解型 EAE モデルに ONO-2506 を経口投与し、神経症候ならびに病理学的検討を行った。

方法

動物：① 慢性進行型 EAE モデル作製には C57BL6 マウス 15 匹、② 再発寛解型 EAE モデル作製には NODLT マウス 15 匹を使用した。

EAE モデルの作製：抗原として MOG のアミノ酸配列 35－55 残基に相当する合成ペプチド（MOG_{35-55}）を用い、EAE を誘導した。100 μg/マウスを両側の鼡径部皮下に分注、接種した。神経症候は臨床スコアを用い、抗原接種当日より 60 日間、連続観察した。観察終了後に H-E 染色と髄鞘染色（K-B 染色）で病理学的検討を行った。

ONO-2506 の経口投与：マウスの口腔から胃ゾンデを挿入し、ONO-2506 を経口投与した。ONO-2506 投与量は既知の実験結果から 30mg/kg/日とした。

① 慢性進行型 EAE モデルは、ONO-2506 30mg/kg/日を抗原接種当日から 30 日間連日または隔日投与した。

② 再発寛解型 EAE モデルは、ONO-2506 30mg/kg/日を抗原接種当日から 30 日間（初回の寛解まで）あるいは 60 日間（再発の寛解まで）連日または隔日投与した。

結果

① 慢性進行型 EAE モデルの検討（C57BL6 マウス）：

神経症候の検討では、ONO-2506 連日・隔日投与群は EAE 群に比べ抗原接種後の神経症候の発現が遅延し、平均臨床スコアの低下を認めた（図１）。病理学的検討では、ONO-2506 連日・隔日投与群は EAE 群に比べ脳・脊髄ともに総計病巣数の減少を認めた（図２）。

② 再発寛解型 EAE モデルの検討（NODLT マウス）：

1）ONO-2506 の 60 日間投与群：神経症候の検討では、ONO-2506 連日・隔日投与群は EAE 群に比べ抗原接種後の神経症候の発現が遅延し、初回および再発時における平均臨床スコアの低下を認めた（図 1 右）。病理学的検討では、ONO-2506 連日・隔日投与群は EAE 群と比べ比べ脳・脊髄ともにに総計病巣数の減少を認めた（図３.左）。

2）ONO-2506 の 30 日間投与群：神経症候の検討では、ONO-2506 連日・隔日投与群は EAE 群に比べ初回の神経症候の発症を抑制し、再発の発症を遅延した。また、再発時における平均臨床スコアの低下を認めた（図１）。病理学的検討では、ONO-2506 連日・隔日投与群は EAE 群に比べ比べ総計病巣数は低下したが、60 日投与群よりも病巣数は多かった（図３.右）。

結論

慢性進行型ならびに再発寛解型 EAE モデルでは、ONO-2506 の 30mg/kg/日の連日または隔日経口投与により EAE の神経症候ならびに再発が抑制され、病理組織学的にも総計病巣数の減少を認めた。以上の結果より、ONO-2506 は、多発性硬化症の再発・進行を抑制する経口薬となる可能性が示唆された。

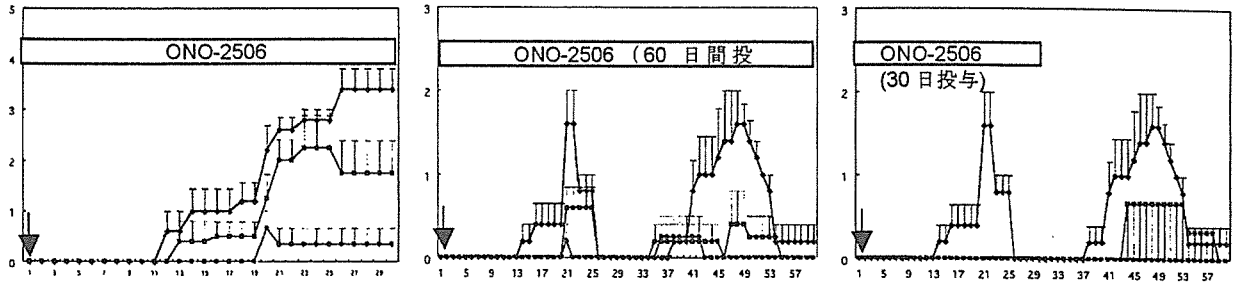

図 1. 慢性進行型・再発寛解型 EAE モデル（■：ONO2506連日投与群、●：隔日投与群、◆：EAE 群）

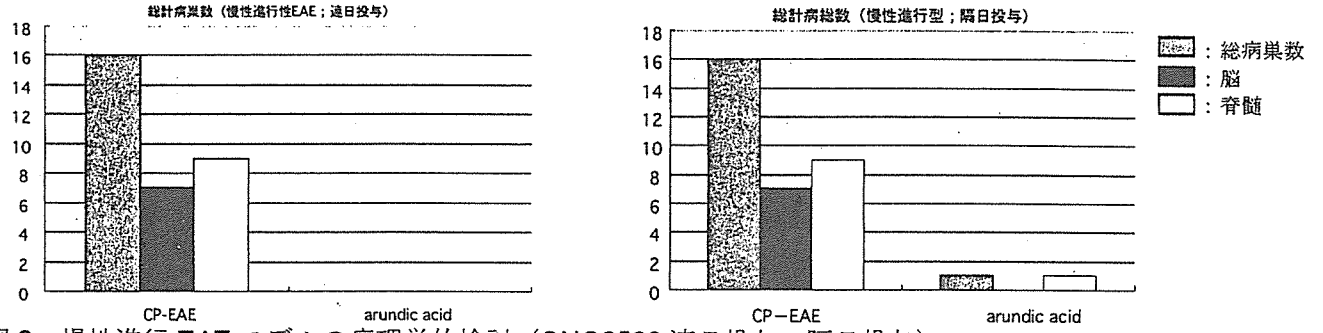

図 2. 慢性進行 EAE モデルの病理学的検討（ONO2506 連日投与、隔日投与）

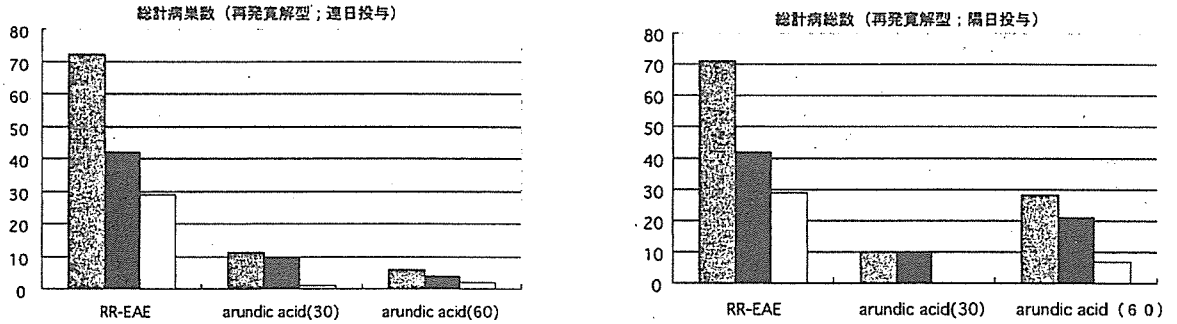

図 3. 再発寛解型 EAE モデルの病理学的検討（ONO2506 連日投与、隔日投与）

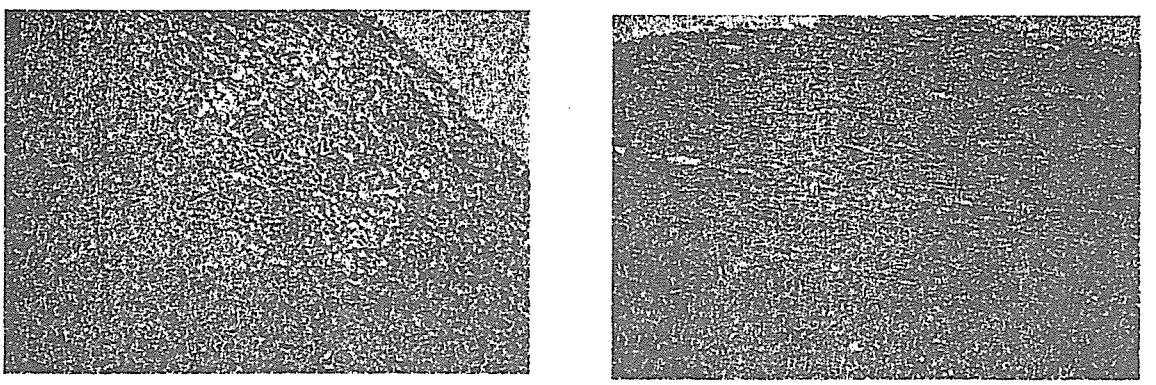

再発寛解型 EAE 群　　ONO2506(30 日間)投与群

図 4. 再発寛解型 EAE モデルの病理組織像　頚髄縦断面 HE 染色 100 倍像

実験的自己免疫性脳脊髄炎の中枢神経における aquaporin-4 の検討

分担研究者： 楠　　進、 研究協力者： ○宮本　勝一
所属施設： 近畿大学医学部神経内科

目的

視神経脊髄型多発性硬化症の多くの例で NMO-IgG が陽性であり、その対応抗原が aquaporin-4 water channel （AQP4）であることが報告されている（J Exp Med, 202:473-7, 2005)。AQP4 は中枢神経だけではなく腎や胃粘膜にも存在する水輸送に関連する水チャネル分子である。脳では脳内水調節に関与し脳浮腫病態との関連が推定されている。脳損傷モデルマウスでは、損傷部での組織浸透圧上昇に伴い、アストロサイトの AQP4 発現が増加し、水分子移動を加速させ脳浮腫病態を悪化させることが明らかになっている。本研究では、多発性硬化症の動物モデルである実験的自己免疫性脳脊髄炎（EAE）における AQP4 の動態を解析する。

方法

C57/B6 マウスに MOG_{35-55} ペプチドを用いて EAE を誘導し、脳・脊髄における AQP4 を定量 PCR を用いて mRNA レベルで評価した。同じコロニーの 6 匹のマウスを 1 セットとし、EAE 誘導前、誘導後 7 日目、14 日目、21 日目、28 日目、35 日目に各 1 匹から脳、脊髄、血液等を採取した。全体で 5 セットのサンプルを得た。AQP4-mRNA は脳、脊髄各々から cDNA を合成し、Realtime-PCR 法（Lightcycler）を用いて定量を行った。また大脳と脊髄の凍結切片を作成し、病理学的に評価した。

結果

EAE 誘導とともに AQP4-mRNA が上昇し、脊髄では誘導後 14 日目に、大脳では 21 日目にピークとなった。凍結切片では、脳、脊髄とも EAE 誘導後 21 日目で脱髄や細胞浸潤が最も著しかった。

考察

EAE の脳、脊髄において AQP4-mRNA の増加が見られた。急性脳虚血モデルでは AQP4 ノックアウトにより脳浮腫が著しく軽減されるという報告があり、EAE の病態においても、AQP4 の発現亢進は炎症巣での浮腫を増強させている可能性がある。一方で AQP-4 の発現亢進は浮腫を軽減させる方向に働く可能性もある。今回明らかになった AQP-4 の動態の意義の解明には今後のさらなる検討が必要である。

Ⅴ．研究成果の刊行に関する一覧表

研究成果の刊行に関する一覧表

書籍

著者氏名	論文タイトル名	書籍全体の編集者名	書籍名	出版社名	出版地	出版年	ページ
Satoh J	Protein Microarray Analysis for Rapid Identification of 14-3-3 Protein Binding Partners.	Predki PF.	Functional Protein Microarrays in Drug Discovery	CRC Press	Boca Raton, FL	2007	235-255
Yamamura.T	Invariant NKT cells and immune regulation in multiple sclerosis.	Jingwu Zhang	In Immune Regulation and Immunotherapy in Autoimmune Disease.	Springer	New York, USA	2007	139-151
Yamamura. T, and Aranami.T	NK cells express a biomarkerler of multiple sclerosis CD11c.	Takeshi Tabira	Current Topics in Neuroimmunology	Medimond Prress	Italy	2007	in press

雑誌

発表者氏名	論文タイトル名	発表誌名	巻号	ページ	出版年	
Satoh J, Nanri Y, Yamamura T	Rapid identification of 14-3-3-binding proteins by protein microarray analysis.	Journal of Neuroscience Methods	152(1-2)	278-288	2006	★
Satoh J, Nakanishi M, Koike F, Onoue H, Aranami T, Yamamoto T, Kawai M, Kikuchi S, Nomura K, Yokoyama K, Ota K, Saito T, Ohta M, Miyake S, Kanda T, Fukazawa T, Yamamura T	T cell gene expression profiling identifies distinct subgroups of Japanese multiple sclerosis patients	J.Neuroimmunol	174(1-2)	108-118	2006	★
Satoh J, Nanri Y, Tabunoki H, Yamamura T	Microarray analysis identifies a set of CXCR3 and CCR2 ligand chemokines as early IFN β-responsive genes in peripheral blood lymphocytes: an implication for IFN β-related adverse effects in multiple sclerosis.	BMC Neurology	6	18-34	2006	★
Miyamoto K, Miyake S, Mizuno M, Oka N, Kusunoki S, Yamamura T.	Selective COX-2 inhibitor celecoxib prevents experimental autoimmune encephalomyelitis through COX-2 independent pathway.	Brain	129	1984-1992	2006	★
Croxford,J.L., S.Miyake, Y-Y,Huang, M.Shimamura, and T.Yamamura	"Invariant V α 19i T cells regulate autoimmune inflammation.	Nat.Immunol	7	987-94	2006	★
Aranami.T,S.Miyake,and T.Yamamura	Differential expression of CD11c by peripheral blood NK cells reflects temporal activity of multiple sclerosis.	Journal of Immunology	177	5659-5667	2006	★
Taro Hino,Takanori Yokota,Shingo Ito,Kazutaka Nishina,Youn-Soo Kang,Shinobu Mori,Satoko Hori,Takashi Kanda,Tetsuya Terasaki,Hidehiro Mizusawa	In vivo delivery of small intefering RNA targeting brain capillary endothelial cells.	Biochem Biophys Res Commun	340	263-267	2006	★
Tomoko Fujita, Naotomo Kambe, and Takashi Uchiyama and Toshiyuki Hori.	Type I interferons attenuate T cell activating functions of human mast cells by decreasing TNF-a production and OX40 ligand expression while increasing IL-10 production.	J. Clin. Immunol.	26	512-518	2006	★

Toshio Kitawaki, Norimitsu Kadowaki, Naoshi Sugimoto, Naotomo Kambe, Toshiyuki Hori, Yoshiki Miyachi, Tatsutoshi Nakahata, Takashi Uchiyama	IgE-activated mast cells in combination with pro-inflammatory factors induce Th2-promoting dendritic cells.	Int. Immunol.	18	1789-1799	2006	★
Ogasawara K, Lanier L L	NKG2D in NK and T cell-mediated Immunity	J. Clin. Immunol.	25	534-540	2005	★
Satoh J, Tabunoki H, Nanri Y, Arima K, Yamamura T	Human astrocytes express 14-3-3 sigma in response to oxidative and DNA-damaging stresses.	Neuroscience Research	56(1)	61-72	2006	
Toshiyuki Hori	Roles of OX40 in the pathogenesis and control of diseases.	Int. J. Hematol.	83	17-22	2006	
Tomoko Fujita, Naoya Ukyo, Toshiyuki Hori, and Takashi Uchiyama	Functional characterization of OX40 expressed on human CD8+ T cells.	Immunol. Lett.	106	27-33	2006	
Yasushi Matsubara, Toshiyuki Hori, Rimpei Morita, Shimon Sakaguchi, and Takashi Uchiyama	Delineation of immunoregulatory properties of adult T cell leukemia cells.	Int. J. Hematol.	84	63-69	2006	
Masahiro Kawahara, Toshiyuki Hori, Yasushi Matsubara, Katsuya Okawa, and Takashi Uchiyama.	Identification of HLA class I-restricted tumor-associated antigens in adult T cell leukemia cells by mass spectrometric analysis.	Exp. Hematol.	34	1496-1504	2006	
Kaida K, Kanzaki M, Morita D, Kamakura K, Motoyoshi K, Hirakawa M, Kusunoki S.	Anti-ganglioside complex antibodies in Miller Fisher syndrome.	J Neurol Neurosurg Psychiatry	77	1043-1046	2006	
Fukazawa T, Kikuchi S, Miyagishi R, Miyazaki Y, Yabe I, Hamada T, Sasaki H	HLA-DPB1*0501 is not uniquely associated with opticospinal multiple sclerosis in Japanese patients. Important role of DPB1*0301	Mult Scler	12	19-23	2006	
Yamagishi S, Kikuchi S, Nakamura K, Matsui T, Takeuchi M, Inoue H	Pigment epithelium-derived factor (PEDF) blocks angiotensin II -induced T cell proliferation by suppressing autocrine production of interleukin-2	Medicinal Chemistry	2(3)	265-269	2006	
Burwick R M, Ramsay P P, Haines J L, Hauser S L, Oksenberg J R, Pericak-Vance M A, Schmidt M, Compston A, Sawcer S, Cittadella R, Savettieri G, Quattrone A, Polman C H, Uitdehaag B M J, Zwemmer J N P, Hawkins C P, Ollier W E R, Weatherby S, Enzinger C, Fazekas F, Schmidt H, Schmidt R, Hillert J, Masterman T, Hogh P, Niino M, Kikuchi S, Maciel P, Santos M, dite Rio M, Kwiecinski H, Zakrzewska-Pniewska B, Evangelou N, Palace J,	APOE epsilon variation in multiple sclerosis and disease severity: some answers	Neurology	66(9)	1378-1383	2006	
Satoh J, Nakanishi M, Koike F, Onoue H, Aranami T, Yamamoto T, Kawai M, Kikuchi S, Nomura K, Yokoyama K, Ota K, Saito T, Ohta M, Miyake S, Kanda T, Fukazawa T, Yamamura T	T cell gene expression profiling identifies distinct subgroups of Japanese multiple sclerosis patients	J. Neuroimmunol	174(1-2)	108-118	2006	
Yamagishi S, Kikuchi S, Nakamura K, Matsui T, Makino T, Norisugi O, Shimizu T, Inoue H, Imaizumi T	Pigment epithelium-derived factor (PEDF) blocks angiotensin II -induced T cell adhesion to endothelial cells by suppressing intercellular adhesion molecule-1	Horm Metab Res	38(8)	546-548	2006	

Taro Hino,Takanori Yokota,Shingo Ito,Kazutaka Nishina,Youn-Soo Kang,Shinobu Mori,Satoko Hori,Takashi Kanda,Tetsuya Terasaki,Hidehiro Mizusawa	In vivo delivery of small intefering RNA targeting brain capillary endothelial cells.	Biochem Biophys Res Commun	340	263-267	2006	
Fujiwara N, Hidano S, Mamada H, Ogasawara K, Kitamura D, Cooper MD, Hozumi N, Chen CL, Goitsuka R	A novel avian homologue of CD72, chB1r, down modulates BCR-mediated activation signals	Int Immunol	18	775-783	2006	
Nomura K, Mitsui T, Okuma A, Kinoshita S, Tomioka R, Takasago Y	Tacrolimus treatment in chronic inflammatory demyelinating polyneuropathy refractory to intravenous immunoglobulin and serum cytokines	Neurology		in press	2006	
Satoh J, Tabunoki H, Yamamura T, Arima K, Konno H.	TROY and LINGO-1 expression in astrocytes and macrophages/microglia in multiple sclerosis lesions.	Neuropathology and Applied Neurobiology	33	99-107	2007	★
Onoue H, Satoh J, Ogawa M, Tabunoki H, Yamamura T	Detection of anti-Nogo receptor autoantibody in the serum of multiple sclerosis and controls.	Acta Neurologica Scandinavica	115	153-160	2007	★
Kuroda R, Satoh J, Yamamura T, Anezaki T, Terada T, Yamazaki K, Obi T, Mizoguchi K.	A novel compound heterozygous mutation in the DAP12 gene in a patient with Nasu-Hakola disease.	Journal of the Neurological Sciences	251(1)	88-91	2007	
Kaida K, Morita D, Kanzaki M, Kamakura K, Motoyoshi K, Hirakawa M, Kusunoki S.	Anti-ganglioside complex antibodies associated with severe disability in GBS.	J. Neuroimmunol	182	212-218	2007	
Fukazawa T, Kikuchi S	A three-dimensional approach for understanding the spectrum of idiopathic inflammatory demyelinating disorders : Importance of the "attack-related severity axis"	Mult Scler		in press	2007	
Ai Kotani, Toshiyuki Hori, Tomoko Fujita, Naotomo Kambe, Yumi Matsumura., Takayuki Ishikawa., Yoshiki Miyachi, Kenichi Nagai, Yuetsu Tanaka, and Takashi Uchiyama	Involvement of OX40 ligand+ mast cells in chronic GVHD after allogeneic hematopoietic stem cell transplantation.	Bone Marrow Transpl.		In press		
Yamamura T	Interleukin 17-producing T-helper cells and autoimmune diseases: Time for a paradigm shift?	Current Rheumatology Reports		in press	2007	
Miyake. S and T. Yamamura	NKT cells and autoimmune diseases:Unraveling the complexity.	Current Topics in Microbiology and Immunology		in press	2007	
Satoh J, Tabunoki H, Yamamura T, Arima K, Konno H.	Human astrocytes express aquaporin-1 and aquaporin-4 in vitro and in vivo.	Neuropathology		in press	2007	
野村恭一	多発性硬化症に対する血液浄化療法	日本医事新報	4255	89	2005	
小笠原康悦,藤原成芳	自己免疫性糖尿病におけるNK活性化レセプターNKG2D	感染　炎症　免疫	36	60-62	2006	

大橋高志、太田宏平、清水優子、大原久仁子、竹内千仙、岩田誠	多発性硬化症におけるインターフェロンβ-1b療法の外来導入の実際	東京女子医科大学雑誌	76	205	2006	
清水優子、太田宏平、川畑仁人、大原久仁子,大橋高志、岩田誠	多発性硬化症における調節性T細胞とFOXP3 mRNA発現の検討（第２報）	神経免疫学	14	49	2006	★
大橋高志、太田宏平、清水優子、大原久仁子、竹内千仙、岩田誠	多発性硬化症における免疫吸着療法の実際	神経免疫学	14	52	2006	★
荒浪利昌, 山村　隆	多発性硬化症の病態　免疫調節機構の破綻	医学のあゆみ	219	125-128	2006	★
佐藤準一	網羅的遺伝子発現解析による多発性硬化症の病態・薬物反応性. 特集II 遺伝子チップ解析の現状とその将来に期待される展開	炎症と免疫	14	205-216	2006	★
佐藤準一	多発性硬化症のマイクロアレイ診断. 特集II 多発性硬化症研究・治療の現状2006.	神経研究の進歩	50	582-599	2006	★
佐藤準一	多発性硬化症. インターフェロン治療学. 最新の基礎・臨床.	日本臨床	64	1297-1309	2006	★
三宅幸子	多発性硬化症における免疫制御細胞の役割とその賦活法. 特集II 多発性硬化症研究・治療の現状2006.	神経研究の進歩	50	636-643	2006	★
南里悠介、佐藤準一、佐藤和貴郎、山村　隆	DNAマイクロアレイによる多発性硬化症の診断とインターフェロンベータ治療反応性予測に関するアンケート調査.	神経内科	64(3)	319-320	2006	
王子 聡, 三井隆男, 吉田典史, 山里将瑞, 大熊 彩, 高濱美里, 島津智一, 大貫 学, 富岳 亮,　松村 治, 野村恭一.	多発性硬化症に対する免疫吸着療法の治療メカニズム	神経免疫学	2006.03. 14巻(1号)	53	2006	
神田　隆	末梢性ニューロパチー、軸索再生、血液神経関門	末梢神経	17	153-159	2006	
荒浪　利昌、山村　隆	NK細胞サブセットと難治性自己免疫疾患	実験医学		in press	2007	

★・・・VI.研究成果の刊行物・別刷に掲載

VI. 研究成果の刊行物・別刷

ELSEVIER

Journal of Neuroscience Methods 152 (2006) 278–288

JOURNAL OF NEUROSCIENCE METHODS

www.elsevier.com/locate/jneumeth

Rapid identification of 14-3-3-binding proteins by protein microarray analysis

Jun-ichi Satoh [a,b,*], Yusuke Nanri [a], Takashi Yamamura [a]

[a] *Department of Immunology, National Institute of Neuroscience, NCNP, 4-1-1 Ogawahigashi, Kodaira, Tokyo 187-8502, Japan*
[b] *Department of Bioinformatics and Neuroinformatics, Meiji Pharmaceutical University, 2-522-1 Noshio, Kiyose, Tokyo 204-8588, Japan*

Received 8 June 2005; received in revised form 19 September 2005; accepted 26 September 2005

Abstract

The 14-3-3 protein family consists of acidic 30-kDa proteins composed of seven isoforms in mammalian cells, expressed abundantly in neurons and glial cells of the central nervous system (CNS). The 14-3-3 isoforms form a dimer that acts as a molecular adaptor interacting with key signaling components involved in cell proliferation, transformation, and apoptosis. Until present, more than 300 proteins have been identified as 14-3-3-binding partners, although most of previous studies focused on a limited range of 14-3-3-interacting proteins. Here, we studied a comprehensive profile of 14-3-3-binding proteins by analyzing a high-density protein microarray using recombinant human 14-3-3 epsilon protein as a probe. Among 1752 proteins immobilized on the microarray, 20 were identified as 14-3-3 interactors, most of which were previously unreported 14-3-3-binding partners. However, 11 known 14-3-3-binding proteins, including keratin 18 (KRT18) and mitogen-activated protein kinase-activated protein kinase 2 (MAPKAPK2), were not identified as a 14-3-3-binding protein. The specific binding to 14-3-3 of EAP30 subunit of ELL complex (EAP30), dead box polypeptide 54 (DDX54), and src homology three (SH3) and cysteine rich domain (STAC) was verified by immunoprecipitation analysis of the recombinant proteins expressed in HEK293 cells. These results suggest that protein microarray is a powerful tool for rapid and comprehensive profiling of 14-3-3-binding proteins.

Keywords: 14-3-3-Binding protein; Immunoprecipitation; Protein microarray; Protein–protein interaction; STAC

1. Introduction

The 14-3-3 protein family consists of evolutionarily conserved, acidic 30-kDa proteins composed of seven isoforms named β, γ, ε, ζ, η, θ, and σ in mammalian cells. A homodimeric or heterodimeric complex composed of the same or distinct isoforms constitutes a large cup-like structure possessing an amphipathic groove with two ligand-binding capacity (Fu et al., 2000; van Hemert et al., 2001). The dimeric complex acts as a molecular adaptor that interacts with key signaling molecules involved in cell differentiation, proliferation, transformation, and apoptosis. It regulates the function of target proteins by restricting their subcellular location, bridging them to modulate catalytic activity, and protecting them from dephosphorylation or proteolysis (Dougherty and Morrison, 2004; MacKintosh, 2004). Although 14-3-3 is widely distributed in neural and non-neural tissues, it is expressed most abundantly in neurons in the central nervous system (CNS), where it represents 1% of total cytosolic proteins (Berg et al., 2002). Aberrant expression and impaired function of 14-3-3 in the CNS are associated with pathogenetic mechanisms of Creutzfeldt–Jacob disease, Alzheimer disease, Parkinson disease, spinocerebellar ataxia, amyotrophic lateral sclerosis, and multiple sclerosis (Chen et al., 2003; Kawamoto et al., 2002; Layfield et al., 1996; Malaspina et al., 2000; Satoh et al., 2004; Zerr et al., 1998).

In general, the 14-3-3 protein interacts with phosphoserine-containing motifs of the ligands such as RSXpSXP (mode I) and RXXXpSXP (mode II) in a sequence-specific manner (Dougherty and Morrison, 2004; MacKintosh, 2004). Previously, more than 300 proteins have been identified as being 14-3-3-binding partners. They include key signaling components, such as Raf-1 kinase, Bcl-2 antagonist of cell death (BAD), protein kinase C (PKC), phophatidylinositol 3-kinase (PI3K), and cdc25 phosphatase (Fu et al., 2000; van Hemert et al., 2001). Binding of 14-3-3 to Raf-1 is indispensable for its kinase activity in the Ras-MAPK signaling pathway, and the interaction of 14-3-3 with BAD, when phosphorylated by

* Corresponding author. Tel.: +81 42 341 2711; fax: +81 42 346 1753.
E-mail address: satoj@ncnp.go.jp (J.-i. Satoh).

0165-0270/$ – see front matter © 2005 Elsevier B.V. All rights reserved.
doi:10.1016/j.jneumeth.2005.09.015

a serine/threonine kinase Akt, inhibits apoptosis. Recent studies indicate that the 14-3-3 protein could interact with a set of target proteins in a phosphorylation-independent manner (Dai and Murakami, 2003; Henriksson et al., 2002; Zhai et al., 2001). Increasing knowledge of interactions between 14-3-3 and interacting molecules would help us to understand the biological function and pathological implication of the 14-3-3 protein networks.

The yeast two-hybrid (Y2H) system is a powerful approach to identify novel protein–protein interactions. However, Y2H screening requires a lot of time and effort, and is often criticized for detecting the interactions unrelated to the physiological setting and obtaining high rates of false positive interactors caused by spontaneous activation of reporter genes and self-activating bait proteins (Vidalain et al., 2004; Zhang et al., 2004). Affinity purification coupled with mass spectrometry (APMS) is an alternative approach to identify the components of protein complexes on a large scale. This approach has been taken to identify a wide variety of 14-3-3-interacting proteins involved in cell proliferation, metabolism, and survival (Benzinger et al., 2005; Jin et al., 2004; Meek et al., 2004; Pozuelo Rubio et al., 2004). Although the APMS procedure detects binding partners of physiological significance, it is laborious and has a difficulty in detecting transmembrane proteins and loosely associated components that might be lost during purification (von Mering et al., 2002). Recently, protein microarray technology has been established for rapid, systematic, and less expensive screening of thousands of protein–protein, protein–lipid, and protein–nucleic acid interactions in a high-throughput fashion. This approach has important applications in the areas not only of basic biological research but also of drug discovery research, including identification of the substrates of protein kinases and the protein targets of small molecules (Chan et al., 2004; MacBeath and Schreiber, 2000; Michaud et al., 2003; Zhu et al., 2001).

The present study was designed for the first time to identify a comprehensive profile of human 14-3-3-binding proteins by analyzing a high-density protein microarray.

2. Materials and methods

2.1. Preparation of a probe for microarray analysis

Human embryonic kidney cells HEK293 whose genome was modified for the Flp-In system (Flp-In 293) were obtained from Invitrogen, Carlsbad, CA. Flp-In 293 cells contain a single Flp recombination target (FRT) site targeted for the site-specific recombination, integrated in a transcriptionally active locus of the genome, where it stably expresses the *lacZ*-Zeocin fusion gene driven from the pFRT/*lac*Zeo plasmid under the control of SV40 early promoter. Flp-In 293 cells were maintained in Dulbecco's modified Eagle's medium (DMEM) supplemented with 10% fetal bovine serum (FBS), 100 U/ml of penicillin, and 100 μg/ml of streptomycin (feeding medium) with inclusion of 100 μg/ml of Zeocin (Invitrogen) as described previously (Satoh and Yamamura, 2004).

To prepare the probe for protein microarray analysis, the open reading frame (ORF) of the human 14-3-3ε gene (YWHAE) was amplified from cDNA of NTera2-N cells (Satoh and Kuroda, 2000) by PCR using PfuTurbo DNA polymerase (Stratagene, La Jolla, CA, USA) and the primer sets listed in Table 1. The PCR product was then cloned into a mammalian expression vector pSecTag/FRT/V5-His TOPO (Invitrogen) to produce a fusion protein with a C-terminal V5 (GKPIPNPLLGLDST) tag, a C-terminal polyhistidine (6 × His) tag, and an N-terminal Ig κ-chain secretion signal. This vector, together with the Flp recombinase expression vector pOG44 (Invitrogen), was transfected in Flp-In 293 cells by Lipofectamine 2000 reagent (Invitrogen). A stable cell line was established after incubating the transfected cells for approximately 1 month in the feeding medium with inclusion of 100 μg/ml of Hygromycin B (Invitrogen). It was named 293 eV5. The recombinant protein was secreted into the culture medium of 293 eV5 cells after the Ig κ-chain secretion signal sequence was processed by an endogenous signal peptidase-mediated cleavage.

To purify the recombinant 14-3-3ε protein, the culture supernatant of 293 eV5 cells incubated for 48 h in the serum-free DMEM/F-12 medium was harvested and concentrated at an 1/40 volume by centrifugation on an Amicon Ultra-15 filter (Millipore, Bedford, MA). It was then purified by the HIS-select spin column (Sigma, St. Louis, MO) and concentrated at an 1/10 volume by centrifugation on a Centricon-10 filter (Millipore). The protein concentration was determined by a Bradford assay kit (BioRad, Hercules, CA). The purity and specificity of the probe were verified by Western blot analysis using mouse monoclonal anti-V5 antibody (Invitrogen) and rabbit polyclonal antibody specific for the 14-3-3ε isoform (IBL, Gumma, Japan).

2.2. Protein microarray analysis

ProtoArray human protein microarray (v1.0) commercially available from Invitrogen was utilized in the present study. It contains 1752 human proteins of various functional classes spotted in duplicate on a nitrocellulose-coated glass slide. To prepare target proteins immobilized on the microarray, an N-terminal glutathione-*S* transferase (GST)-6 × His fusion protein derived from the genes selected from the human ultimate ORF clone collection (Invitrogen) was expressed in Sf9 insect cells by using the baculovirus expression system (Invitrogen). Either the full-length or the partial fragment of recombinant proteins, was purified under native conditions by glutathione affinity chromatography in the presence of protease inhibitors, then processed for spotting on the slides. The proteins were printed in an arrangement composed of 4 × 12 subarrays equally spaced in vertical and horizontal directions (Fig. 1a). Each subarray included 16 × 16 spots, composed of 48 control spots (C), 80 human proteins (H), and 128 blanks (B) (Fig. 1c). The control proteins (C) were composed of 14 positive control spots and 34 negative control spots. The former includes four spots of an Alexa Fluor 647-labeled antibody (rows 1, 8; columns 1, 2), six spots of a concentration gradient of a biotinlyated anti-mouse antibody with a capacity to bind to mouse monoclonal anti-V5 antibody conjugated with Alexa Fluor 647 (row 8; columns 3–8), and four spots of a concentration gradient of V5 protein (row 8; columns 13–16). The latter includes six spots of

Table 1
Primers utilized for PCR-based cloning and site-directed mutagenesis

Genes	Proteins (amino acid residues)	GenBank accession no.	Sense primers	Antisense primers	Cloning vector
YWHAE	14-3-3ε Isoform (2-255)	NM_006761	5′gatgatcgaggaggatctggtgtac3′	5′ctgattttcgtctttccacgtcctg3′	pSecTag/FRT/V5-His TOPO
EAP30	EAP30 subunit of ELL complex (2-258)	NM_007241	5′caccgccgcgggatggaggctggc3′	5′tcaggaggaggctctctgccttc3′	pcDNA4/HisMax-TOPO
DDX54	Dead box polypeptide 54 (2-881)	NM_024072	5′gcggcgacaaggccggcggct3′	5′tcacatcctcttccgcatcttgcc3′	pcDNA4/HisMax-TOPO
STAC	src homology three and cysteine rich domain (2-402, full length)	NM_003149	5′atcccctcgagcagccccgcgag3′	5′tcagatgtttctagtacatcaag3′	pcDNA4/HisMax-TOPO
STAC	src homology three and cysteine rich domain (2-402 with S172A; SMT)	NM_003149	5′gtttcggcgttactacgcctcccccttgctcatttc3′	5′gaatgagcaaggggaggcgtagtaacgccgaaac3′	pcDNA4/HisMax-TOPO modified by site-directed mutagenesis
STAC	src homology three and cysteine rich domain (2-402 with S172A and S173A; DMT)	NM_003149	5′cggcgttactacgccgccccttgctcatttcat3′	5′atgaatgagcaaggggcggcgtagtaacgccg3′	pcDNA4/HisMax-TOPO modified by site-directed mutagenesis
STAC	src homology three and cysteine rich domain (2-233, N-terminal half; NTF)	NM_003149	5′atcccctcgagcagccccgcgag3′	5′tcaaagatctgaagtagaggttct3′	pcDNA4/HisMax-TOPO
STAC	src homology three and cysteine rich domain (234-402, C-terminal half; CTF)	NM_003149	5′gtggaggttcctgaggaagccaat3′	5′tcagccacctggatgcagaccagc3′	pcDNA4/HisMax-TOPO
STAC	src homology three and cysteine rich domain (2-164, truncated form A; TR-A)	NM_003149	5′atcccctcgagcagccccgcgag3′	5′tcatggcagcttgcccatgcaccg3′	pcDNA4/HisMax-TOPO
STAC	src homology three and cysteine rich domain (2-105, truncated form B; TR-B)	NM_003149	5′atcccctcgagcagccccgcgag3′	5′tcagccacctggatgcagaccagc3′	pcDNA4/HisMax-TOPO

The PCR product was cloned into a vector pSecTag/FRT/V5-His TOPO to express a fusion protein with a V5 tag or into a vector pcDNA4/HisMax-TOPO to express a fusion protein with a Xpress tag in HEK293 cells.

a concentration gradient of bovine serum albumin (BSA) (row 1; columns 3–8), four spots of a concentration gradient of a rabbit anti-GST antibody (row 1; columns 9–12), four spots of a concentration gradient of calmodulin (row 1; columns 13–16), 16 spots of a concentration gradient of GST (row 2; columns 1–16), two spots of buffer only (row 8; columns 9,10), and two spots of an anti-biotin antibody (row 8; columns 11,12). The complete list of 1752 target proteins immobilized on the microarary is shown in Supplementary Table 1 online.

Non-specific binding was blocked by incubating the microarray for 90 min in the PBST blocking buffer composed of 1% BSA and 0.1% Tween 20 in phosphate-buffered saline (PBS). Then, it was incubated for 30 min at 4 °C with the probe described above at a concentration of 50 μg/ml in the probing buffer composed of 1% BSA, 5 mM $MgCl_2$, 0.5 mM dithiothreitol (DTT), 0.05% Triton X-100, and 5% glycerol in PBS. The array was washed three times with the probing buffer, followed by incubation for 30 min at 4 °C with mouse monoclonal anti-V5 antibody conjugated with Alexa Fluor 647 (Invitrogen) at a concentration of 260 ng/ml in the probing buffer. The array was washed three times with the probing buffer, and then scanned by the GenePix 4200A scanner (Axon Instruments, Union City, CA) at a wavelength of 635 nm. The data were analyzed by using the ProtoArray Prospector software v2.0 (Invitrogen) following acquisition of the microarray lot-specific information online, including inter-lot variations in protein concentrations (http://www.invitrogen.com/protoarray). According to the default setting of the software, the spots showing the background-subtracted signal intensity value greater than the median plus three standard deviations of all the fluorescence intensities were considered as having a significant binding. The Z-score, an indicator for statistical evaluation of binding specificity, was calculated as the background-subtracted signal intensity value of the target protein minus the average of the background-subtracted signal intensity value from the negative contro distribution, divided by the standard deviation of the negative control distribution. All the procedure described above could be accomplished within 5 h. The 14-3-3-binding consensus motif mode I (RSXpSXP) sequence located in target proteins was surveyed by the Scansite Motif Scanner, which assesses the probability of a site matching the candidate motif under high, medium, or low stringent conditions (Obenauer et al., 2003). The information on known 14-3-3 interactors was obtained from Biomolecular Interaction Network Database (BIND; http://www.bind.ca) and PubMed database search.

2.3. Transient expression of 14-3-3-binding proteins in HEK293 cells

To verify the results of microarray analysis, the ORF of the genes encoding EAP30 subunit of ELL complex (EAP30), dead box polypeptide 54 (DDX54), and src homology three (SH3) and cysteine rich domain (STAC) were amplified by PCR using PfuTurbo DNA polymerase and the primer sets listed in Table 1. They were then cloned into a mammalian expression vector pcDNA4/HisMax-TOPO (Invitrogen) to produce a fusion protein with an N-terminal Xpress tag. To express the STAC mutant

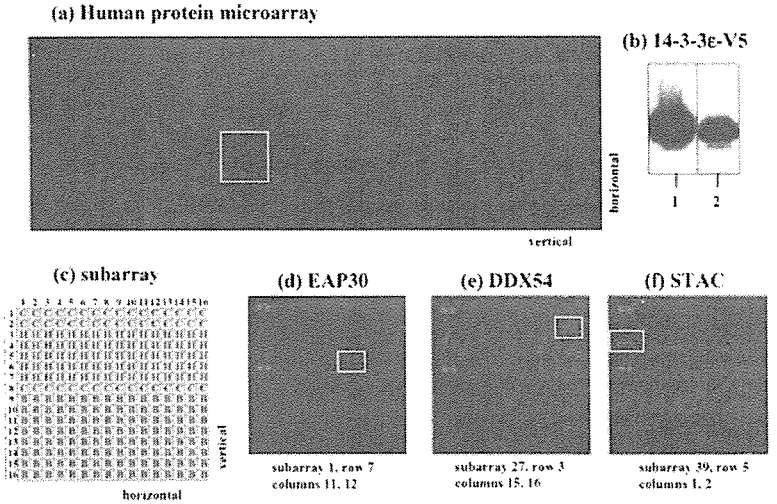

Fig. 1. Protein microarray analysis. (a) Human protein microarray. The microarray contains 1752 distinct human proteins of various functional classes spotted in duplicate on a nitrocellulose-coated glass slide. They are printed in an arrangement of 4 × 12 subarrays equally spaced in vertical and horizontal directions. A representative subarray is indicated by an enclosed yellow line. (b) Recombinant human 14-3-3ε protein tagged with V5. One microgram of the protein was processed for Western blot analysis using anti-V5 antibody (lane 1) or anti-14-3-3ε antibody (lane 2). (c) Layout of the subarray. Each subarray includes 16 × 16 spots composed of 48 control spots (C), 80 human proteins (H), and 128 blanks (B). The positive control spots include an Alexa Fluor 647-labeled antibody (rows 1, 8; columns 1, 2; strong signals), a concentration gradient of a biotinylated anti-mouse antibody with a capacity to bind to mouse monoclonal anti-V5 antibody conjugated with Alexa Fluor 647 (row 8; columns 3–8; signals visible on the higher concentration), and a concentration gradient of V5 protein (row 8; columns 13–16; signals visible on the higher concentration). (d) EAP30. (e) DDX54. (f) STAC. The three proteins indicated by an enclosed yellow line located on different subarrays (d–f) represent an example identified as showing significant binding to the probe.

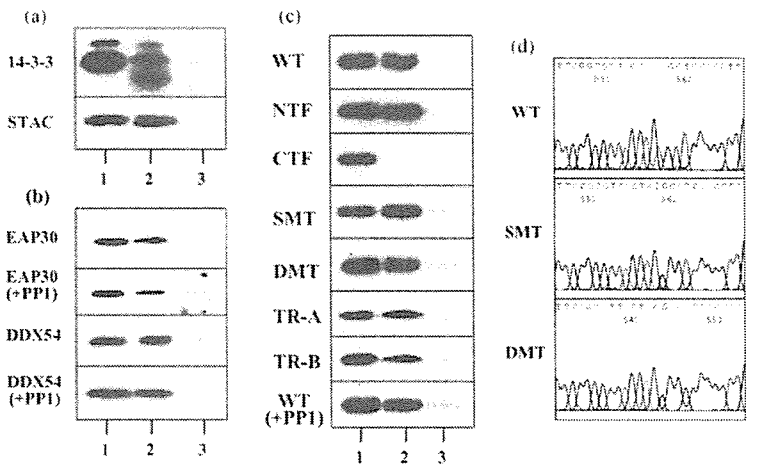

Fig. 2. Immunoprecipitation analysis of 14-3-3-binding proteins. (a) Binding of STAC to 14-3-3. Total protein extract of HEK293 cells expressing Xpress-tagged recombinant STAC was processed for immunoprecipitation (IP) with rabbit polyclonal antibody reacting with all 14-3-3 isoforms (K-19) or with normal rabbit IgG. The immunoprecipitates were then processed for Western blot analysis using mouse monoclonal antibody reacting with all 14-3-3 isoforms (H-8) (upper panel) or mouse monoclonal anti-Xpress antibody (lower panel). Lanes (1–3) represent (1) the input control, and IP with (2) K-19 and (3) normal rabbit IgG. (b) Binding of EAP30 and DDX54 to 14-3-3. Total protein of HEK293 cells expressing Xpress-tagged recombinant EAP30 or DDX54 extracted by using the lysis buffer with inclusion of phosphatase inhibitors or with inclusion of protein phosphatase-1 (PP1) instead of phosphatase inhibitors (+PP1) was processed for IP with K-19 or with normal rabbit IgG. The immunoprecipitates were then processed for Western blot analysis using anti-Xpress antibody. Lanes (1–3) represent (1) the input control, and IP with (2) K-19 and (3) normal rabbit IgG. (c) Binding of mutant and truncated STAC to 14-3-3. Total protein was extracted from HEK293 cells expressing a panel of Xpress-tagged recombinant STAC proteins. They include the full-length wild-type (WT) STAC, the N-terminal half (NTF), the C-terminal half (CTF), the S172A mutant (SMT), the S172A and S173A double mutant (DMT), the truncated form lacking the 14-3-3-binding consensus motif RYYSSP (TR-A), the truncated form lacking the cysteine-rich domain (CRD) (TR-B), and WT STAC isolated by using the lysis buffer with inclusion of PP1 instead of phosphatase inhibitors (WT + PP1). Primers utilized for PCR-based cloning and site-directed mutagenesis are listed in Table 1. The lysate was processed for IP with K-19 or with normal rabbit IgG. The immunoprecipitates were then processed for Western blot analysis using anti-Xpress antibody. Lanes (1–3) represent (1) the input control, and IP with (2) K-19 and (3) normal rabbit IgG. (d) The sequence of the 14-3-3-binding consensus motif located in amino acid residues 169-174 in expression vectors of STAC. The panels indicate WT (nucleotide sequence CGT-TAC-TAC-AGC-TCC-CCC: the corresponding amino acid sequence RYYSSP), SMT (CGT-TAC-TAC-GCC-TCC-CCC: RYYASP), and DMT (CGT-TAC-TAC-GCC-GCC-CCC: RYYAAP).

with a single amino acid substitution S172A (the single mutant; SMT) or with double amino acid substitutions S172A and S173A (the double mutant; DMT), the pcDNA4/HisMax-TOPO vector containing the wild-type (WT) STAC gene was modified by consecutive site-directed mutagenesis using QuikChange II site-directed mutagenesis kit (Stratagene) and the primer sets listed in Table 1. The mutations introduced in the vector were verified by sequencing analysis (Fig. 2d). All these vectors were transfected in HEK293 cells by Lipofectamine 2000 reagent.

2.4. Immunoprecipitation analysis

To prepare total protein extract, the cells were homogenized and incubated at room temperature for 30 min in M-PER lysis buffer (Pierce, Rockford, IL) supplemented with a cocktail of protease inhibitors (Sigma), with inclusion of phosphatase inhibitors (Sigma) to maintain the protein phosphorylation status or with inclusion of recombinant protein phosphatase-1 (PP1) catalytic subunit α-isoform (5 U/ml; Sigma) instead of phosphatase inhibitors to induce the protein dephosphorylation reaction (Ichimura et al., 2005), followed by centrifugation at 12,000 rpm at 4 °C for 20 min. After preclearance, the supernatant was incubated at 4 °C for 3 h with 30 μg/ml rabbit polyclonal anti-14-3-3 protein antibody (K19)-conjugated agarose (Santa Cruz Biotechnology, Santa Cruz, CA) or the same amount of normal rabbit IgG-conjugated agarose (Santa Cruz Biotechnology). After several washes, the immunoprecipitates were processed for Western blot analysis using mouse monoclonal anti-14-3-3 protein antibody (H-8, Santa Cruz Biotechnology) and mouse monoclonal anti-Xpress antibody (Invitrogen). K-19 and H-8 antibodies recognize all 14-3-3 isoforms. The specific reaction was visualized using a chemiluminescent substrate (Pierce).

3. Results

3.1. Protein microarray analysis identified 20 distinct 14-3-3-binding partners

To analyze a high-density human protein microarray, the recombinant 14-3-3ε protein tagged with V5 was purified form the supernatant of 293 eV5 cells secreting the recombinant protein in the culture medium. Western blot analysis verified the purity and specificity of the probe (Fig. 1b). Among 1752 proteins on the microarray, 20 were identified as the proteins showing significant binding to the probe (Table 2). All of these were previously unreported 14-3-3-binding partners by the BIND search. Seven were hypothetical clones of uncharacterized function, derived from the mammalian genome collection (MGC) or the full-length long Japan (FLJ). Thirteen annotated proteins included EAP30 subunit of ELL complex (EAP30) (Fig. 1d), lymphocyte cytosolic protein 2 (LCP2), methionine aminopeptidase 2 (METAP2), melanoma antigen family B, 4 (MAGEB4), chondroitin 4 sulfotransferase 11 (CHST11), nuclear interacting partner of anaplastic lymphoma kinase (ZC3HC1), minichromosome maintenance deficient 10 (MCM10), DEAD box polypeptide 54 (DDX54) (Fig. 1e), heterogeneous nuclear ribonucleoprotein C (HNPRC), fibroblast growth factor 12 (FGF12), glutathione *S*-transferase M3 (GSTM3), src homology three (SH3) and cysteine rich domain (STAC) (Fig. 1f), and ATPase, H+ transporting, lysosomal, 21 kDa, V0 subunit C″ (ATP6V0B). The 14-3-3-binding consensus motif mode I (RSX*p*SXP) was found only in STAC (*pS*172) and HNRPC (*pS*125) by the Scansite Motif Scanner search under the high stringent condition, while 15 of 20 proteins have one or several motifs when a query with the medium or low stringency was performed (Table 2).

3.2. Immunoprecipitation analysis validated the specific binding to 14-3-3

EAP30, DDX54, and STAC were selected to verify the results of microarray analysis, in view of their higher Z-scores. The recombinant proteins were expressed in HEK293 cells, which constitutively express a substantial amount of endogenous 14-3-3 protein. Total protein was extracted by using the lysis buffer with inclusion of phosphatase inhibitors to maintain the protein phosphorylation status or with inclusion of recombinant protein phosphatase-1 (PP1) instead of phosphatase inhibitors to induce the protein dephosphorylation reaction, followed by processing for immunoprecipitation (IP) with rabbit polyclonal antibody reacting with all 14-3-3 isoforms (K-19) or with normal rabbit IgG. K19 coimmunoprecipitated 14-3-3 and STAC from the lysate of HEK293 cells expressing the recombinant STAC protein, whereas normal rabbit IgG did not pull down these proteins (Fig. 2a). K-19 immunoprecipitated EAP30 and DDX54 from the lysate of HEK293 cells expressing the recombinant EAP30 or DDX54 protein, respectively, under both phosphorylated and dephosphorylated conditions (Fig. 2b). These results indicate that EAP30, DDX54, and STAC could interact with the endogenous 14-3-3 protein in HEK293 cells where the corresponding recombinant proteins were expressed.

STAC has the highly stringent 14-3-3-binding consensus motif RYYSSP in amino acid residues 169-174 (*pS*172), as suggested by the Scansite Motif Scanner (Table 2). Therefore, a possible involvement of this motif in binding to 14-3-3 was investigated by IP analysis of a series of mutant and truncated STAC proteins (Table 1). K-19 immunoprecipitated the full-length wild-type (WT) STAC comprised of amino acid residues 2-402 (Fig. 2a and c). K-19 also pulled down the S172A mutant (SMT), and the S172A and S173A double mutant (DMT), and the N-terminal half (NTF; amino acid residues 2-233) from the lysate of HEK293 cells expressing the corresponding recombinant proteins (Fig. 2c). In contrast, K-19 did not pull down the C-terminal half (CTF; amino acid residues 234-402) (Fig. 2c). These observations indicate that the RYYSSP motif is not essential for binding of STAC to 14-3-3. This was confirmed by the observations that K-19 immunoprecipitated the truncated form lacking the RYYSSP sequence (TR-A; amino acid residues 2-164) and the shortest form lacking both the RYYSSP sequence and the cysteine-rich domain (CRD) (TR-B; amino acid residues 2-105) from the lysate of HEK293 cells expressing the corresponding recombinant proteins (Fig. 2c). Finally, the full-length WT STAC interacted with 14-3-3 under the dephosphorylated condition (Fig. 2c). These observations indicate that the

Table 2
Twenty 14-3-3-binding proteins identified by protein microarray analysis

No.	Symbol	Database ID	Protein name	Putative biological function	14-3-3-binding consensus motif mode I	Stringency level of the binding motif	Subarray	Row	Column	Z-score
1	EAP30	NM_007241	EAP30 subunit of ELL complex	a 30-kDa component of the ELL complex that confers derepression of transcription by RNA polymerase II	No sites	NA	1	7	11	22.8593
									12	24.60829
2	FLJ10415	NM_018089	Hypothetical protein, cDNA clone MGC:969	Unknown	S258: ARGGPSHSAGANLRR	Low	5	4	11	4.16265
					S405: SPKQGSGSEGEDGFQ	Low			12	4.35203
					S525: PADPRVLSLLSAPLG	Low				
					S690: VNTRRCWSCGASLQG	Low				
3	LOC57228	NM_020467	Hypothetical protein	Unknown	S28: AARKRNISSNDSQAP	Low	5	6	9	16.84741
									10	17.1519
4	MGC17403	NM_152634	Hypothetical protein	Unknown	T274: KQLRASYTESCIQEH	Low	11	3	1	4.04754
									2	4.08838
5	LCP2	NM_005565	Lymphocyte cytosolic protein 2	A 72-kDa protein (SLP76) that associates with the Grb2 adaptor protein, provides a substrate of the ZAP-70 protein tyrosine kinase, and plays a role in promoting T cell development and activation	S297: TTERHERSSPLPGKK	Low	13	5	11	4.47457
					S376: SSFPQSASLPPYFSQ	Low			12	4.46343
					T456: DSSKKTTTNPYVLMV	Low				
6	METAP2	NM_006838	Methionine aminopeptidase 2	A 67-kDa protein that interacts with eukaryotic initiation factor-2 (eIF-2) and regulates protein synthesis	T113: KRGPKVQTDPPSVPI	Low	15	6	11	3.54252
					S152: TAAWRTTSEEKKALD	Low			12	3.31601
7	MAGEB4	NM_002367	Melanoma antigen family B, 4	A member of the MAGEB family expressed in testis whose function remains unknown	T18: AREKRQRTRGQTQDL	Medium	18	3	7	9.50614
					T194: GNQSSAWTLPRNGLL	Low			8	9.30562
					S339: SAYSRATSSSSSQPM	Low				
8	CHST11	NM_018413	Chondroitin 4 sulfotransferase 11	A member of HNK-1ST family GalNAc 4-O-sulfotransferase that plays a role in chondroitin sulfate and dermatan sulfate biosynthesis	S93: TDTCRANSATSRKRR	Medium	20	5	3	3.97327
					S56: DICCRKGSRSPLQEL	Low			4	3.92871
					S194: EPFERLVSAYRNKFT	Low				
9	ZC3HC1	NM_016478	Nuclear interacting partner of anaplastic lymphoma kinase (ALK)	A 60-kDa protein that interacts with ALK and plays an antiapoptotic role in nucleophosmin-ALK signaling events	No sites	NA	23	3	3	3.33458
									4	3.55366

Table 2 (*Continued*)

No.	Symbol	Database ID	Protein name	Putative biological function	14-3-3-binding consensus motif mode 1	Stringency level of the binding motif	Subarray	Row	Column	Z-score
10	MCM10	NM_018518	Minichromosome maintenance deficient 10	A key component of the pre-replication complex (pre-RC) that is essential for the initiation of DNA replication	S90: AQPPRTGSEFPRLEG	Medium	25	3	13	4.26291
					S35: KPAIKSISASALLKQ	Low			14	4.12552
					S55: LEMRRRKSEEIQKRF	Low				
					S302: PCGNRSISLDRLPNK	Low				
					T329: DGMLKEKTGPKIGGE	Low				
11	DDX54	NM_024072	DEAD (Asp-Glu-Ala-Asp) box polypeptide 54	A 97-kDa RNA helicase (DP97) that interacts with estrogen receptor (ER) and represses the transcription of ER-regulated genes	T95: EDKKKIKTESGRYIS	Low	27	3	15	9.2425
					S102: TESGRYISSSYKRDL	Low			16	9.10882
12	HNPRC	NM_004500	Heterogeneous nuclear ribonucleoprotein C	A member of heterogeneous nuclear ribonucleoproteins (hnRNPs) involved in pre-mRNA processing, mRNA metabolism and transport	S125: DYYDRMYSYPARVPP	High	28	6	9	4.81248
					S158: NTSRRGKSGFNSKSG	Low			10	5.18382
					S170: KSGQRGSSKSGKLKG	Low				
					S240: ETNVKMESEGGADDS	Low				
13	LOC137781	BC032347	Hypothetical gene, cDNA clone MGC:40429	Unknown	No sites	NA	30	5	11	3.56109
									12	3.47568
14	LOC92345	NM_138386	Hypothetical protein	Unknown	S339: QGRKKLKSEFNEPGE	Low	32	5	13	3.55366
					T374: GYRNREFTRGFSRAR	Low			14	3.73933
					S467: PLLNLPYSLPPPPPP	Low				
15	FGF12	NM_004113	Fibroblast growth factor 12, transcript variant 2	A member of the FGF family that plays a role in nervous system development and function	S150: VCMYREQSLHEIGEK	Low	34	6	5	5.73339
					S165: QGRSRKSSGTPTMNG	Low			6	5.75567
16	GSTM3	NM_000849	Glutathione *S*-transferase M3 (brain)	A cytoplasmic glutathione *S*-transferase of the mu class that plays a role in detoxification of carcinogens, therapeutic drugs, environmental toxins, and products of oxidative stress	S64: GIKLRSFSV	Low	38	5	15	7.82029
									16	7.70889
17	STAC	NM_003149	src homology three (SH3) and cysteine rich domain	A 47-kDa protein with a SH3 and a cysteine-rich domain that plays a role in the neuron-specific signal transduction pathway	S172: KGFRRYYSSPLLIHE	High	39	5	1	16.63575
					S56: TKSLRSKSADNFFQR	Medium			2	16.64318
					S255: DLRKRSNSVFTYPEN	Medium				
					S46: QKLKRSLSFKTKSLR	Low				
					S51: SLSFKTKSLRSKSAD	Low				
					S66: NFFQRTNSEDMKLQA	Low				
					S253: GYDLRKRSNSVFTYP	Low				